Journal of Sol-Gel Science and Technology 37, 31–37, 2006

DOI: 10.1007/s10971-005-5062-2

Low-Temperature Sol-Gel Synthesis of Single-Phase $ZrTiO_4$ Nanoparticles

I.C. COSENTINO, E.N.S. MUCCILLO AND R. MUCCILLO*
Centro Multidisciplinar para o Desenvolvimento de Materiais Cerâmicos CCTM—Instituto de Pesquisas Energéticas e Nucleares, C.P. 11049 S. Paulo, SP, Brazil 05422-970
muccillo@usp.br

F.M. VICHI
Laboratório de Química de Materiais e Energia, Depto. de Química Fundamental, Instituto de Química, Universidade de S. Paulo, Av. Prof. Lineu Prestes 748 S. Paulo, SP, Brazil 05508-000

Received February 14, 2005; Accepted September 16, 2005

Published online: 2 January 2006

Abstract. Ceramic $ZrTiO_4$ powders were prepared by a sol-gel method using zirconium oxychloride and titanium tetraisopropoxide. *In situ* high temperature X-ray diffraction results show that crystallization of the amorphous gel starts at 400 °C. Single-phase $ZrTiO_4$ nanoparticles were obtained after heat treatment at 450 °C for one hour. An average particle size of 46 nm has been determined by nitrogen adsorption analysis. After pressing these sinteractive powders, pellets with controlled pore size distribution were obtained by sintering at temperatures as low as 400 °C. The analysis of pores by mercury porosimetry gives an average porosity of 45%. The electrical resistivity, determined by impedance spectroscopy measurements at 24 °C under different humidity environments, shows the ability of these pellets to adsorb water vapor in the porous surfaces. Pellets fabricated with the nanosized powders prepared by the sol-gel technique are proposed as good candidates to be used in humidity sensing devices.

Keywords: sol-gel process, porous ceramics, zirconia-titania

1. Introduction

Ceramic materials based on zirconium titanate ($ZrTiO_4$) are extensively used in humidity sensors [1–3], resonators for microwave telecommunications [4–6], catalysis [7–9], and optical devices [10]. Other materials, based on zirconium titanate, have found applications as high temperature pigments and ceramic composites [11]. Titanate-based compounds have also been considered for use as ceramic matrices for the disposal of surplus nuclear weapons material [12–14]. It has been shown that mixed TiO_2-ZrO_2 binary oxides exhibit higher photocatalytic activity than pure TiO_2 [15, 16]. Crystal structure studies have shown that $ZrTiO_4$ presents the orthorhombic structure [17], and at temperatures above 1200 °C $ZrTiO_4$ has the α-PbO_2 structure (space group Pcnb) with a total disordering of Ti^{4+} and Zr^{4+} cations occupying the available octahedral sites [13, 18]. Classical $ZrTiO_4$ synthesis involves a solid state reaction of a stoichiometric mixture of zirconium and titanium oxides at temperatures above 1400 °C [19], and more recently the preparation of agglomerated 0.5–3.0 μm single phase $ZrTiO_4$ particles at 1300 °C from the precursor oxides [20]. Solid state reactions involve grinding and thorough mixing of precursor powders followed by high temperature prolonged sintering; the results are usually low specific surface area powders. These powders, upon pressing and sintering, result in non homogeneous rather dense materials lacking the necessary porosity for humidity sensing devices. The sol-gel technology may overcome these problems because highly sinteractive (high specific surface area) powders may be prepared, requiring much lower sintering temperature [21]. The sol-gel technique has been widely used to produce ceramic materials which are difficult to obtain by conventional techniques. Detailed descriptions of the sol-gel technique may be found elsewhere [22, 23]. However, it is important to have in mind, when using the sol-gel technique, the control of hydrolysis and condensation rates of the molecular precursors, usually metal alcoxides. For this reason,

*To whom all correspondence should be addressed.

seemingly identical procedures can lead to different materials, and extreme care must be taken when establishing routine procedures. A number of ZrO_2-TiO_2 binary oxides prepared by the sol-gel technique have been reported [24–27]. Fully crystalline and stoichiometric $ZrTiO_4$ have been obtained with a crystallization temperature of 400 °C by preparing TiO_2 and ZrO gels and mixing them on a 1:1 ratio [24]. The low temperature synthesis of $ZrTiO_4$ from different precursors with a Zr:Ti concentration ratio of 1:1 has been reported [26], with $ZrTiO_4$ phase formation around 700 °C. More recently, pure $ZrTiO_4$ phases have been obtained at 650 °C, but the preparation procedure is not clear, and the XRD results are dubious [28]. The preparation of $ZrTiO_4$ at 800 °C for catalysis application, also by a sol-gel method, was recently reported [29]. One of the most common techniques for preparing metal oxides is the polymeric precursor technique [30]. Even though low particle size and sinteractive powders are obtained, high crystallization temperatures are required for $ZrTiO_4$ [31, 32].

With respect to sensitivity to humidity, mixed ZrO_2-TiO_2 binary oxides are comparable to commercial $MgCr_2O_4$-TiO_2 ceramics [32]. The conduction mechanism is not clear, although it has tentatively been related to oxygen vacancies, since doping with MgO and Fe_2O_3, as well as heating in a nitrogen atmosphere, create oxygen vacancies in porous ZrO_2-TiO_2 ceramics [1]. The presence of oxygen vacancies may enhance the adsorption of water at the grain boundaries, in the form of V_O-OH^-, which in turn give rise to mobile protons. The higher the adsorbed water content, the more hydroxyl groups are formed on the surface, increasing the dielectric constant and lowering the dissociation energy. The consequence is an increase in the number of charge carriers [33].

Taking advantage of the sol-gel method, the low temperature preparation of $ZrTiO_4$ ceramic nanoparticles was successfully achieved and is here described. The material was prepared by a modified sol-gel method, in which the titanium alcoxide was hydrolized in the presence of zirconium oxychloride, as opposed to hydrolising in pure acidic water. Our aim using this modified approach is to ensure the maximum contact between titanium and zirconium, thus leading to lower formation temperatures for $ZrTiO_4$. It is shown that the $ZrTiO_4$ phase is obtained in the pure form at 400 °C, and that after pressing and sintering the nanosized particles, the electrical conductivity of the sintered pellets increases with increasing relative humidity. These materials prepared by a sol-gel method are more favorable for applications in humidity sensing devices than the ones obtained by the conventional solid state synthesis for many reasons: the sol-gel material is homogeneous, crystallizes at a lower temperature, and upon pressing and sintering produces ceramic pieces with suitable porosity for use in humidity sensing devices.

2. Experimental

2.1. Ceramic Powder Preparation

The starting materials were a solution of zirconium oxychloride $ZrOCl_2.8H_2O$ and titanium tetraisopropoxide ($Ti[OCH(CH_3)_2]_4$—Alfa Aesar). The zirconium oxychloride, 159 g L^{-1} concentration, was prepared by dissolving, in hydrochloric acid, hydrous zirconium oxide $ZrO_2.nH_2O$ (>99%) produced at IPEN-Brazil. For the preparation of 10 g of the ceramic powders in the nominal composition ZrO_2:TiO_2, 14 mL of titanium tetraisopropoxide were slowly added to 39 mL of a zirconium oxychloride solution (pH ∼ 0.5) under continuous stirring at room temperature. The suspension was stirred for approximately seven days. The solution, milky with a white precipitate at the beginning, was translucent, almost transparent after long time stirring. The obtained sol was then transferred to a Petri dish and dried at approximately 40 °C for another seven days. A yellowish transparent glassy material was then obtained (Fig. 1, top) and ground in an agate mortar to obtain the amorphous $ZrTiO_4$ ceramic powder (Fig. 1, bottom). These figures were obtained with a stereoscope optical microscope Nikon model SMZ 800, coupled to a JVC model TK-C1380E digital camera.

Some specimens were also prepared by the polymeric precursor technique and by mixing the oxides. For the polymeric precursor technique, zirconium oxychloride (obtained by adding hydrochloric acid to zirconium oxide produced at this Institute), titanium chloride, 99.5% citric acid and ethylene glycol were used. The powder preparation consists essentially on mixing zirconium oxychloride and titanium chloride on the desired stoichiometry, keeping at 60 °C and adding citric acid. Ethylene glycol is then added and the temperature of the solution is raised to 110 °C for the formation of the polymeric resin. The calcination of the resin is performed in two steps: at 250 °C for 1 h, resulting in a brownish glassy powder, and at 730 °C for 1 h, with a 2 °C min^{-1} rate, yielding a fine white ceramic powder. For the mixing of oxides technique, zirconium oxide and titanium oxide were mixed in a 1:1 molar ratio, pressed at 147 MPa and sintered in air at different temperatures (950, 1050, 1150 and 1250 °C) for obtaining specimens with different pore volume content [3].

2.2. Characterization

The stoichiometry of the powders was analyzed by X-ray fluorescence in a Jordan Valley ED-XRF model Ex-Calibur spectrometer. Standard compositions of $(ZrO_2)_x(TiO_2)_{1-x}$ (x = 0, 0.25, 0.50, 0.75 and 1), both oxides from Alfa Aesar, were prepared by mixing and pressing for XRF

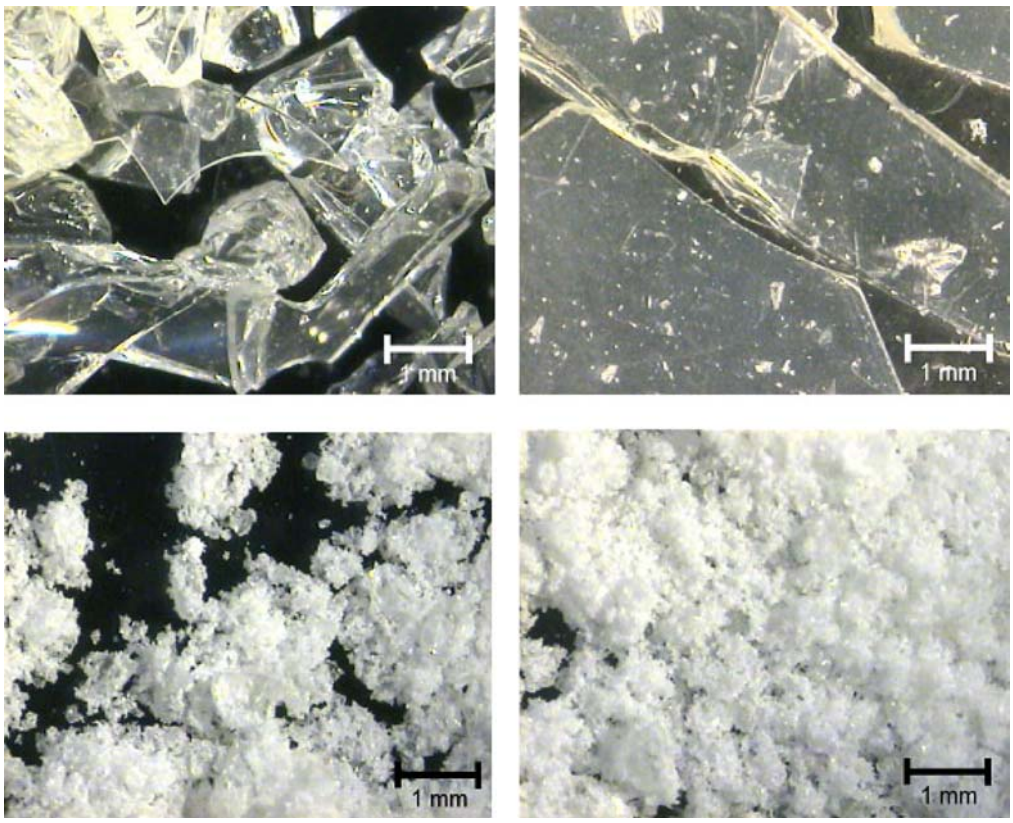

Figure 1. Optical images of the $ZrTiO_4$ prepared by sol-gel technique. Top: as obtained; bottom: after grinding.

measurements to establish a calibration curve. The relative concentrations of Ti and Zr in the powders obtained by the sol-gel technique were determined as 50.1% and 49.9%, respectively.

Thermogravimetric analysis (Shimadzu model TGA-50) was carried out in the dried powder under synthetic air in the room temperature −800 °C range, with a 20 °C min^{-1} heating rate. Differential Scanning Calorimetry analysis (Shimadzu model DSC-50) was carried out in the 25–475 °C at the same rate.

The specific surface area of the powders was evaluated by gas adsorption analysis by the BET method using a Micromeritics ASAP 2000 equipment. For this measurement, the powder was heated under vacuum overnight at approximately 150 °C for elimination of moisture from surfaces and open pores; pure dry nitrogen was the carrier gas.

Scanning electron microscopy experiments were carried out on powder suspensions in a LEO 440 SEM equipment for observing particle shape and to evaluate average particle size.

X-ray diffraction analysis was performed in all powders with CuKα radiation in the 20–80° 2θ range in a Bruker-AXS D8 Advance X-ray diffractometer.The pellets had the diffraction measurements performed in the 20–50° 2θ range on their flat surfaces. High temperature *in situ* X-ray diffraction experiments were performed in air in the same diffractometer in a θ-θ configuration with an Anton Paar high temperature sample chamber and a Braun PSD detector (0.007 2θ step size, 0.0061 s counting time). The sol-gel prepared $ZrTiO_4$ powders were placed on top of a platinum strip to be heated at 4 °C s^{-1} to dwelling temperatures in the room temperature-800 °C range, for measuring the phase evolution from amorphous to crystalline as a function of temperature.

Powder density was evaluated by mercury porosimetry with a Micromeritics Autopore III porosimeter. The pore size distribution and the apparent density of the pellets were evaluated in the 360 μm–0.003 μm (30 Å) range using mercury pressure up to 414 MPa.

For electrical measurements, the powders were pressed into cylindrical pellets and heat treated at 200, 300 and 400 °C for 3 h. The temperature of 300 °C was the lowest that produced pellets with mechanical resistance enabling handling the specimens for electrical measurements and for further use in sensing devices. Therefore, samples heat treated at temperatures of 300 °C and higher were chosen for the study of the dependence of the electrical response on the relative humidity. The electrical characterization of the ceramic pellets was performed by impedance spectroscopy measurements (Hewlett Packard 4192A Impedance Analyzer) over the 5 Hz–13 MHz frequency range at 24 °C. A sample chamber, consisting of a glass cup with a lucite lid and stainless steel feed-thru electrodes, was designed to keep the samples in a constant humidity environment. To improve electrical

contacts, silver electrodes were applied to the flat surfaces of the ceramic pellets by painting with silver paste and curing at 250 °C for 15 min.

3. Results and Discussion

3.1. Powder Analysis

Figure 2 shows the thermogravimetric analysis of the zirconia-titania powder prepared by the sol-gel technique.

A significant mass loss is measured from room temperature to approximately 600 °C due to the removal of water, organic substances, and chloride. The remaining material corresponds to 42.9% of the mass before heating. The mass loss occurs in at least three steps: 33.8% from RT to 384 °C, 20.1% in the 384–417 °C range, and 3.2% in the 417–600 °C range. The sharp feature of the mass loss in the second step might be associated to the exothermic crystallization process. Carefully controlled differential scanning calorimetry experiments, as shown in the inset of Fig. 2, did not allow for determining unambiguously the expected exothermic peak of the crystallization process. High temperature *in situ* X-ray diffraction analysis (see below) helped to determine accurately the crystallization temperature. The temperatures 450 °C and also 600 °C were chosen as calcination temperatures for the powders prepared by the sol-gel technique.

Figure 3 shows X-ray diffraction patterns of the powders obtained by the sol-gel technique after calcination at 450 °C for 1 h (Fig. 3a) and at 600 °C for 1 h (3b). For comparison purposes, the diffraction pattern of a powder obtained by the polymeric precursor technique and calcined at 730 °C for 1 h is also shown (Fig. 3c). The diffraction patterns of Figs. 3a and 3b show that the powders are crystallized in the $ZrTiO_4$ structure according to ICDD file #80-1783. Only the reflections due to the $ZrTiO_4$ phase are identified in powders obtained by the sol-gel technique and calcined at 450 and 600 °C. Similar results are obtained in powders prepared by the polymeric precursor technique. Moreover,

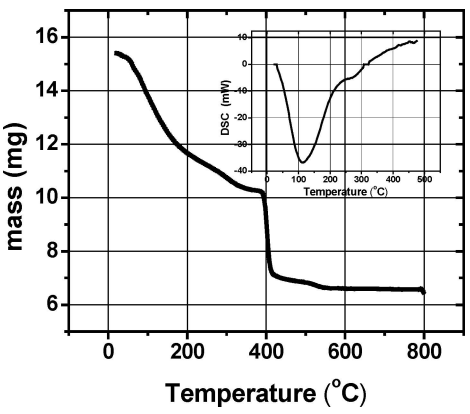

Figure 2. Thermogravimetric analysis of the $ZrTiO_4$ powder prepared by a sol-gel technique and dried at 35 °C; heating rate 20 °C min^{-1}.

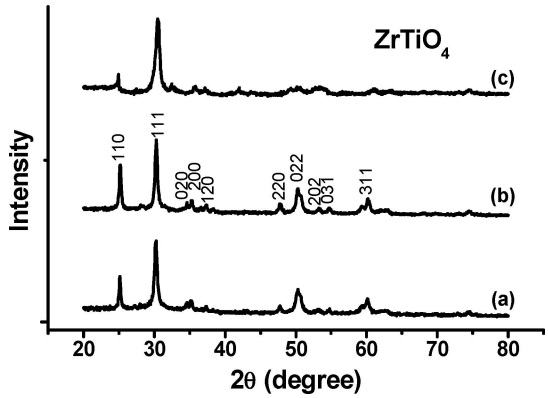

Figure 3. X-ray diffraction patterns of the $ZrTiO_4$ powders obtained by the sol-gel technique and calcined at 450 (a) and 600 °C (b) for 1 h; for comparison purposes, the X-ray diffraction pattern of the powder obtained by the polymeric precursor technique and calcined at 730 °C for 1 h is also shown (c) [3]. Indexation according to ICDD file 80-1783.

the crystallization occurs at a temperature lower than that of the powders obtained by the polymeric precursor technique [3]. Most of the methods for obtaining $ZrTiO_4$ crystalline powders require temperatures close to 700 °C [33].

High temperature X-ray diffraction experiments were performed for crystallization studies. Figure 4 shows the dependence of the intensity of the (111) reflection ($2\theta = 30.498°$, ICDD file # 80-1783) on the temperature upon heating the $ZrTiO_4$ amorphous ceramic powder from 27 °C to 800 °C. Data were collected at the following temperatures: 27, 100, 200, 250, 300, 350, 400 to 500 °C at 10 °C increment, and 550 to 800 °C at 50 °C increment. The heating rate for reaching each temperature was set at 4 °C s^{-1}. The inset shows the (111) reflection at all these temperatures. Figure 4 shows that crystallization starts at approximately 400 °C.

Figures 5a and 5b show the results of the scanning electron microscopy experiments on powders calcined at 450

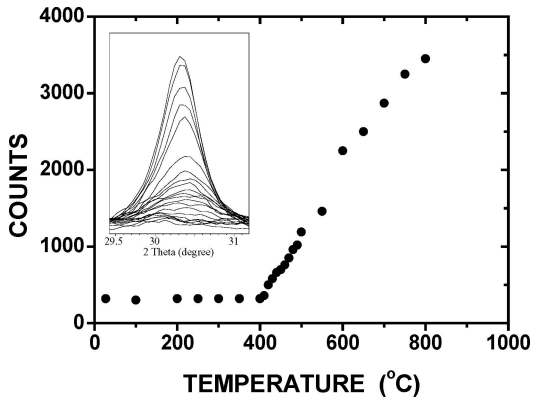

Figure 4. High temperature *in situ* X-ray diffraction data: intensity of the (111) reflection of $ZrTiO_4$ powders obtained by the sol-gel technique as a function of temperature in the 27-800 °C range. Inset: illustration of the (111) reflection at different temperatures from 27 °C (bottom) to 800 °C (top).

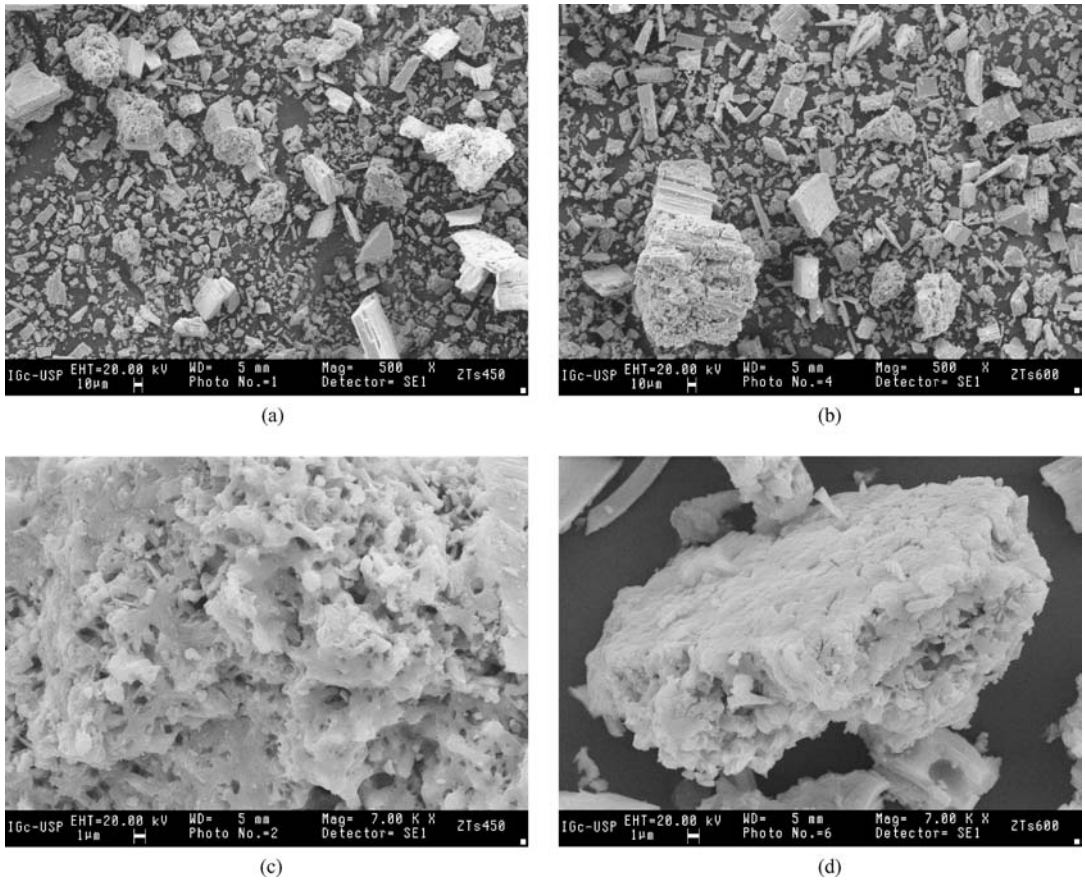

Figure 5. Scanning electron microscopy micrographs of the $ZrTiO_4$ powders obtained by the sol-gel technique: a) calcination temperature 450° C for 1h (500X); b) 600° C for 1 h (500X); c) 450° C for 1 h (7000X); and d) 600° C for 1 h (7000X).

and 600 °C, respectively, for 1 h. Both powders consist of large agglomerates probably resulting from the high combustion heat produced during the thermal decomposition of the powders. Larger magnification of these micrographs, Figs. 5c and 5d, shows that the agglomerates are composed of clusters of submicron sized particles.

A detailed analysis of the powders was done to find the average equivalent diameter of the agglomerated particles. The BET method for the determination of the specific surface area by nitrogen gas adsorption analysis was applied. The results show that the specific surface area of $ZrTiO_4$ powder after calcination at 450 and 600 °C are 43 and 38 m^2 g^{-1}, respectively. Using the equation $D\,(\mu m) = 6/(\rho.S)$, the equivalent spherical diameter of the particles D was evaluated; ρ, determined by mercury porosimetry, and S stand for the $ZrTiO_4$ density (g cm^{-3}) and the specific surface area (m^2 g^{-1}), respectively. These results are shown in Table 1. Particles treated at 450 and 600 °C show no apparent modification in their average size. The specific surface area shows a slight decrease with consequent increase in the apparent density and in the average size of the particles probably due to particle sintering and pore elimination. Table 1 also shows values of the mean crystallite size L of these powders, determined using the Scherrer equation [34]. The mean crystallite sizes are of the same order of magnitude (approximately half) of the values of the average particle sizes determined by gas adsorption analysis. This means that the nanoparticles obtained by the modified sol-gel technique here described may be single crystalline, provided further cominution of the dried gel is done.

3.2. *Analysis of the Sintered Pellets*

The powders calcined at 600 °C were cold pressed and heat treated at 300 and 400 °C for 3 h. Figure 6 shows the X-ray diffraction patterns of these pellets. There is a partial decomposition of the $ZrTiO_4$ phase to monoclinic zirconia

Table 1. Specific surface area S, apparent density ρ, average equivalent diameter D, and crystallite size L of the powders obtained by the sol-gel technique after calcination at 450 °C and 600 °C.

Temperature of calcination	S (m^2/g)	r (g/cm^3)	D (nm)	L (nm)
450 °C	43	3.00	46.5	20.5
600 °C	38	3.19	49.5	21.5

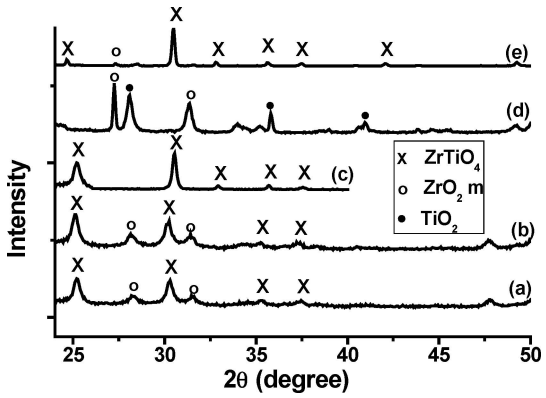

Figure 6. X-ray diffraction patterns of pellets sintered at 300 (a) and 400 °C (b) for 1 h, prepared with powders obtained by a sol-gel technique. Also shown the X-ray diffraction patterns of pellets sintered at 1150 °C for 1 h from powders prepared by the polymeric precursor technique (c) and sintered at 950 °C (d) and 1250 °C (e) for 1 h from powders prepared by the solid state synthesis.

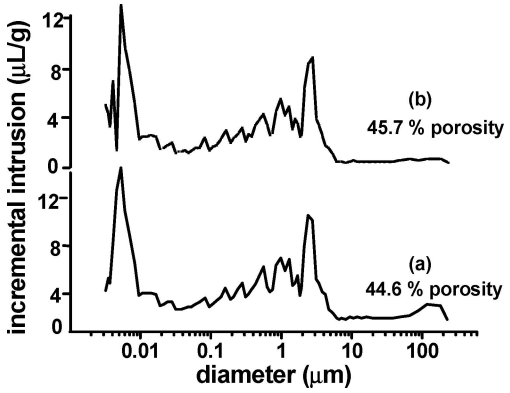

Figure 7. Pore size distribution in ceramic pellets obtained by sintering at 300 and 400 °C for 1 h pressed powders prepared by a sol-gel technique.

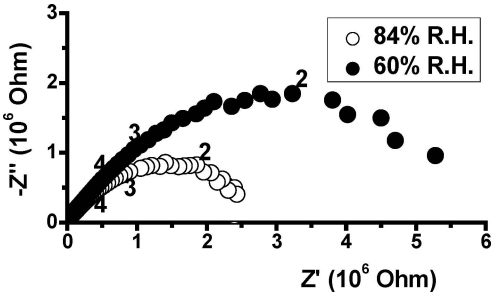

Figure 8. Room temperature impedance diagrams of pellets sintered at 300 °C for 1 h, prepared from powders obtained by a sol-gel technique, at two humidity conditions.

(Figs. 6a and 6b). As the temperature is lower than the calcination temperature, mechanical stresses during pressing could be the main reason for that decomposition. Similar results have been observed in nanosized tetragonal zirconia particles submitted to mechanical stress by grinding [35]. In the same figure, the X-ray diffraction patterns of $ZrTiO_4$ specimens obtained by solid state synthesis (mixing, pressing and sintering), Fig. 6d and 6e, and by the polymeric precursor technique, Fig. 6c, are also shown, for comparison purposes. The pellets prepared using powders obtained by the polymeric precursor technique and sintered at 1150 °C (Fig. 6c) are $ZrTiO_4$ single phase. The pellet obtained by solid state synthesis and sintered at 950 °C has two phases: monoclinic zirconia and rutile TiO_2. The $ZrTiO_4$ phase is found only after sintering at 1050 °C and higher temperatures, becoming $ZrTiO_4$ single phase only after sintering at 1250 °C (Fig. 6e), in agreement with reported results [36].

The application of the $ZrTiO_4$ sintered pellets we are looking for is as humidity sensing main component. Therefore, one of the main requirements is a large distribution of pores for accommodation of water species for changing the electrical resistivity. Figure 7 shows the results of the pore size distribution analysis of the pellets sintered at 300 and at 400 °C, prepared from powders obtained by the sol-gel technique. Pore distribution is about the same for both specimens, with approximately 45% pore volume and similar size distribution. Both specimens have also a large pore density in the region 50–300 Å. This is important for designing ceramic humidity sensors because the larger is the pore density in that range, the better is the linearity and the sensitivity of the sensor [37].

As both specimens had approximately the same pore size distribution, the one sintered at the lower temperature (300 °C / 3 h) was chosen for electrical measurements by the impedance spectroscopy technique. Two were the humidity conditions: under open air (relative humidity 60%), and inside a sample chamber closed with a saturated potassium chloride solution (84%). Figure 8 shows the $[-Z''(\omega) \times Z'(\omega)]$ impedance diagrams of the pellet under 60% and 84% relative humidity, measured at room temperature, in the 5 Hz–13 MHz frequency range. The numbers in the plots represent the logarithm of the frequency of the applied voltage signal (50 mV). Each impedance diagram is composed of one well defined semicircle representing the electrical response of the interfaces (mainly composed of pores). The electric resistance of the specimen is determined by the intercept of the semicircle in the low frequency region of the real axis of the impedance diagram [3]. One can see that the higher is the relative humidity the lower is the value of the electrical resistance. The porous structure of the specimen, determined by mercury porosimetry, adsorbs water molecules yielding hydroxyl groups, which, by their turn, dissociate to produce H^+ charge carriers, responsible for enhancing the electrical conductivity. A detailed analysis of the electrical behavior by the impedance spectroscopy technique will be published elsewhere [38].

4. Conclusions

A successful preparation of clustered nanosized particles of $ZrTiO_4$ ceramic powders by a modified sol-gel technique

allowed for sintering at relatively low temperatures porous ceramic pellets. The crystallization temperature of the powders was accurately determined as 400 °C by *in situ* high temperature X-ray diffraction. The average size values of the nanoparticles is approximately twice that of the crystallite size value. The sol-gel technique is an appropriate technique for preparing sinteractive ceramic nanoparticles for the design of ceramic pieces to be used in humidity sensing devices. The electrical response of the pellets prepared by pressing and sintering nanosized powders prepared by the sol-gel technique showed that these ceramics may be used in humidity sensing devices. The studies on the main requirements for using these pellets in humidity sensors, namely, sensitivity and selectivity to moisture, speed and stability of the electrical signal are under way.

Acknowledgments

To CNEN, FAPESP (99/10798–0 and 98/14324–0), CNPq (RM: Proc. 306496/88, ENSM: Proc. 300934/94-7) and PRONEX for financial support. To O. Vercino and Y. V. França for thermal analysis measurements and to I. Sayeg (Instituto de Geociências—USP) for SEM analysis.

References

1. S. Yang and J.M. Wu, J. Mater. Sci. **26**, 631 (1991).
2. M. K. Jain, M. C. Bhatnagar, and G. L. Sharma, Sens. Actuators B **55**, 17 (1999).
3. I.C. Cosentino, E.N.S. Muccillo, and R. Muccillo, Sens. Actuators B **96**, 677 (2003).
4. K. Wakino, H. Minai, and H. Tamura, J. Am. Ceram. Soc. **67**, 278 (1984).
5. M. Leoni, M. Viviani, G. Battilana, A.M. Fiorello, and M. Viticoli, J. Eur. Ceram. Soc. **21**, 1739 (2001).
6. A.J. Moulston and J.M. Herbert, *Electroceramics* (Chapman & Hall, New York, 1990).
7. F.P. Daly, H. Ando, J.L. Schmitt, and A.E. Sturm, J. Catal. **108**, 401 (1987).
8. J. Miciukiewicz and T. Mang, Appl. Catal. A: Gen. **122**, 151 (1995).
9. B.M. Reddy, P.M. Sreekanth, Y. Yamada, Q. Xu, and T. Kobayashi, Appl. Catal. A: Gen. **228**, 28 (2002).
10. D.A. Chang, P. Lin, and T. Tseng, J. Appl. Phys. **77**, 4445 (1995).
11. F.Z. Hund, Z. Anorg. Allg. Chem. **525**, 221 (1985).
12. W. Lutze and R.C. Ewing, *Radioactive Waste Forms for the Future* (North Holland, New York, 1988).
13. W. Lutze, R.C. Ewing and W.J. Weber, *Disposal of Weapons Plutonium* (Kluwer, Netherlands, 1996).
14. W. Lutze and R.C. Ewing, J. Mater. Res. **10**, 243 (1995).
15. X. Fu, L.A. Clark, and M.A. Anderson, Environ. Sci. Technol. **30**, 647 (1996).
16. J.C. Yu, J. Lin, and R.M.W. Kwok, J. Phys. Chem. B **102**, 5094 (1998).
17. R.E. Newnham, J. Am. Ceram. Soc. **50**, 216 (1967).
18. A. Harari, J. Bocquet, M. Huber, and R.C. Collongues, C. R. Acad. Sci. Ser. C. **267**, 1316 (1968).
19. A.E. McHale and R.S. Roth, J. Am. Ceram. Soc. **69**, 827 (1986).
20. S. Ananta, R. Tipakontitikul, and T. Tunkasiri, Mater. Lett. **57**, 2637 (2003).
21. J.A. Navio, F.J. Marchena, M. Macias, P.J. Sanchez-Soto, and P. Pichat, J. Mater. Sci. **27**, 2463 (1992).
22. C.J. Brinker and G.W. Scherer, *Sol-Gel Science: The Physics and Chemistry of Sol-Gel Processing* (Academic Press, San Diego, 1990).
23. L.L. Hench and J.K. West, Chem. Rev. **90**, 33 (1990).
24. A.K. Bhattacharya, K.K. Malick, A. Hartridge, and J.L. Woodhead, Mater. Lett. **18**, 247 (1994).
25. A.K. Bhattacharya, K.K. Mallick, A. Hartridge, and J.L. Woodhead, J. Mater. Sci. **31**, 267 (1996).
26. E.L. Sham, M.A.G. Aranda, E.M. Farfa-Torres, J.C. Gottifredi, M. Martinez-Lara, and S. Bruque, J. Solid State Chem. **139**, 225 (1998).
27. M. Adrianainarivelo, R.J.P. Corriu, D. Lechlercq, P.H. Mutin, and A. Vious, J. Mater. Chem. **7**, 279 (1997).
28. L.G. Karakchiev, T.M. Zima, and N. Lyakhov, Z. Inorg. Mater. **37**, 386 (2001).
29. H. Zou and Y.S. Lin, Appl. Catal. A: Gen. **265**, 35 (2004).
30. S. Yamamoto, M. Kakihana, and S. Kato, J. Alloys Comp. **297**, 81 (2000).
31. P.R. de Lucena, O.D. Pessoa-Neto, I.M.G. dos Santos, A.G. Souza, E. Longo, and J.A. Varela, J. Alloys Comp. **397**, 255 (2005).
32. T. Nitta, Z. Terada, and S. Hayakawa, J. Am. Ceram. Soc. **63**, 295 (1980).
33. S.-L Yang and J.-M. Wu, J. Mater. Sci. **26**, 631 (1991).
34. B.E. Warren, *X-Ray Diffraction* (Dover Publications, Inc., New York, 1969) p. 253.
35. N. Claussen and M. Ruhle, in *Advances in Ceramics*, edited by A. H. Heuer and L. W. Hobbs (The American Ceramic Society, Inc., Columbus, 1981), p. 137.
36. F. Khairulla and P.P. Phule, Mater. Sci. Eng. B **12**, 327 (1992).
37. M.K. Jain, M.C. Bhatnagar, and G.L. Sharma, Jpn. J. Appl. Phys. **39**, 345 (2000).
38. I.C. Cosentino, E.N.S. Muccillo, and R. Muccillo (2005) unpublished.